2016 24th International Lightning Detection Conference &
6th International Lightning Meteorology Conference
18 - 21 April | San Diego, California, USA

ATDnet detection efficiency and cloud lightning detection characteristics from comparison with the HyLMA during HyMeX SOP1

Sven-Erik Enno, Graeme Anderson, Jacqueline Sugier
Observations
Met Office
Exeter, United Kingdom
sven-erik.enno@metoffice.gov.uk

***Abstract*— This study provides a detailed quantitative detection efficiency (DE) estimation for the Met Office long-range Very Low frequency (VLF) lightning location system ATDnet. The system is validated against the lightning mapping array deployed in the south of France in autumn 2012 [Rison, 2012] as part of the Hydrological Cycle in the Mediterranean Experiment (HyMeX) project Special Observation Period 1 (SOP1) [Defer et al., 2015].**

The overall ATDnet flash DE was approximately 91% for the 285 ground flashes (CG) and 24% for the 1341 cloud flashes (IC) in three studied storms. For the individual storms CG DE ranged from 86 to 94% and IC DE ranged from 24 to 35%. For 65% of the ICs registered by ATDnet, the preliminary breakdown was detected. ATDnet IC DE was much higher for flashes with larger vertical extent.

Keywords—lightning detection, detection efficiency, ATDnet, HyMeX, lightning mapping array

I. Introduction

High quality real time lightning data are increasingly important for severe weather monitoring and forecasting. Most of the European countries are covered by a lightning location system (LLS), either operated by the National Met Service or by a private company or other organization. There is a trend towards international cooperation of ground based and satellite based (geostationary) lightning detection.

LLSs typically rely on the radio frequency electromagnetic fields produced by lightning. CG flashes contain one or more strokes which involve a downward leader and an upward return stroke. Return strokes are easiest to detect especially at VLF/LF frequency range as they produce reasonably powerful radio emissions [e.g., Nag et al., 2015]. Detected strokes are often grouped into flashes on the basis of predefined spatial and temporal criteria [e.g., Anderson and Klugmann, 2014]. The largest radio emissions of cloud lightning are related to initial breakdown process [Rakov and Uman, 2003].

All LLSs have their limitations and most importantly not all strokes are detected. Detection efficiency (DE) is used to quantify the fraction of detected strokes or flashes compared to the real number of strokes/flashes that occur. Flash DE is likely to be higher than stroke DE as a flash is considered to be detected even if only one stroke of the flash was detected [e.g. Rakov, 2013]. Depending on the nature of the reference data, absolute or relative DE can be reported.

Absolute DE is very difficult to measure, as it requires a reference LLS capable of detecting all flashes or strokes. Relative DE of one system compared to another is calculated by dividing the number of coincident strokes or flashes by the total number detected by the reference network [e.g. Abarca et al., 2010; Lagouvardos et al., 2009].

Ground flashes pose the greatest threat to lives and infrastructure, so CG DE is a critical performance measure. For most of the modern short-range LLSs including EUCLID [Poelman et al., 2013b] and LINET [Betz et al., 2009] in Europe, and the U.S. National Lightning Detection Network (NLDN) [Biagi et al., 2007; Nag et al., 2011] in America, ground flash DE above 90% has been measured in their core regions. IC DE is rarely reported as it can be more difficult to quantify.

There are fewer long-range LLSs than short-range systems: examples include the University of Washington WWLLN (Worldwide Lightning Location Network) system [Lay et al., 2004], the Vaisala GLD360 (Global Lightning Dataset 360) system [Said et al., 2010], the National Observatory of Athens ZEUS network [Lagouvardos et al., 2009], STARNET [Dentel et al., 2014] and the ATDnet system operated by the Met Office. Such systems can cover whole continents as well as seas and oceans that are not observable using short-range networks. This means that they can provide valuable data for intercontinental flight routes, for example. There is also an increased interest in using long-range LLS data for the calibration/validation of geostationary lightning sensors in the future. However, better knowledge of the DE for long-range LLSs is required.

In the present paper the ATDnet flash DE is measured against the HyMeX Lightning Mapping Array (HyLMA). ATDnet is a very low frequency (VLF) long-range LLS operated by the Met Office [Bennett et al., 2011]. During the study period, ATDnet consisted of 11 sensors in and around Europe operating at a central frequency of 13.733 kHz. The effective service area of the system encompasses Europe, Northern Africa, and northern parts of the Atlantic.

ATDnet sensors detect atmospherics (also called sferics). Sferics are electromagnetic waves in the VLF range that propagate in the Earth-ionosphere waveguide and are usually generated by CG return strokes [Rakov and Uman, 2003]. The system takes the advantage of the long propagation paths of sferics which makes it possible to cover large areas with only a limited number of sensors.

ATDnet detections are called “fixes”. Fixes are located using data from a minimum of four ATDnet sensors. The long baselines between ATDnet sensors mean that only relatively powerful emissions will be detected. As CG strokes tend to emit the most powerful sferics in the VLF range, whereas IC processes generally emit weaker sferics [e.g. Cummins and Murphy, 2009], it is often assumed that long-ranges LLSs are only capable of detecting CG lightning.

Studies into other long-range VLF networks have demonstrated recently that this assumption is oversimplified, however, and that VLF networks are in fact capable of detecting some IC lightning [Jacobson et al., 2006; Lagouvardos et al., 2009]. A recent comparison of ATDnet with the Météorage short-range network in France demonstrated that ATDnet detected a large proportion of flashes that the short-range network categorized as ICs [Poelman et al., 2013a], indicating – but not proving – that ATDnet also detects cloud lightning.

Quantitative proof requires direct observation of the lightning channels. This is possible by registering very high frequency (VHF) radio emissions associated with the channel formation process and leader processes in pre-existing channels [Nag et al., 2015].

The best available system for detailed total lightning data with nearly 100% DE is the Lightning Mapping Array (LMA) developed by New Mexico Tech [Rison et al., 1999; Krehbiel et al., 2000]. The LMA detects VHF sources (referred to as sources) in the 60-66 MHz frequency range, with a source location rate of up to more than 10,000 sources per second. The system has three-dimensional location accuracy within the area covered by the array of only a few tens of meters or better. As such, it can be used to reliably map out the three-dimensional development and structure of lightning channels.

As part of the Hydrological Cycle in the Mediterranean Experiment (HyMeX) project [Drobinski et al., 2014], a dedicated LMA (referred to as the HyLMA) was deployed for over two months in the south of France (Fig. 1). The HyLMA consisted of 12 sensors and was operational during the HyMeX Special Observation Period 1 that lasted from 5 September to 6 November 2012 [Defer et al., 2015]. The obtained data could be used as a reliable reference against which LLSs could be validated.

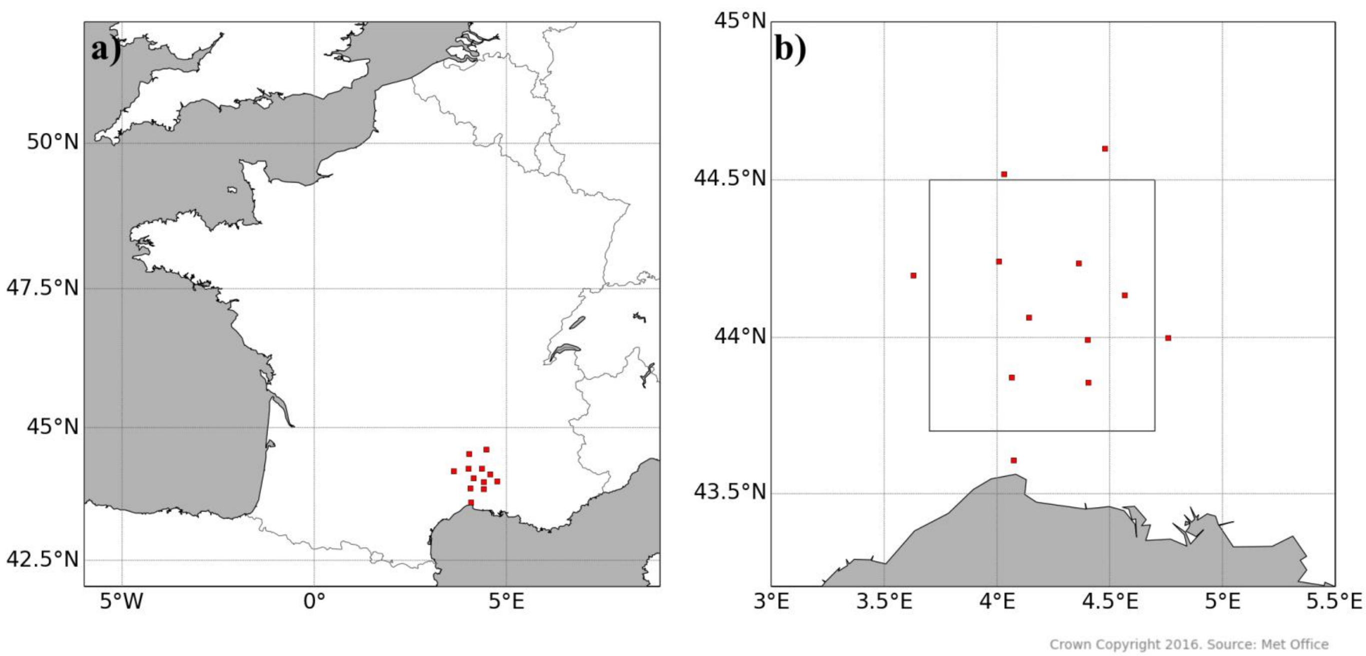

Fig. 1. Locations of the HyLMA sensors as red squares (a) and border of the study area as a black rectangle (b).

The main objective of the present paper is to provide a comprehensive quantitative estimation of ATDnet detection efficiency for different types of flashes. The research carried out by Enno et al. [2016] is expanded and the impact of ATDnet quality control on DE is estimated for the first time.

Section 2 describes the approach used in comparing HyLMA and ATDnet data and Section 3 represents the main results. Section 4 provides a discussion of the results and Section 5 concludes the study.

II. Data and Methods

A. Data

The ATDnet data include a date, time, location (latitude and longitude) and error estimate for each fix. The error estimate is the orientation and length of the major axis and the minor axis of an ellipse in which a fix is located with a 95% probability. No discrimination between IC and CG discharges is provided.

All ATDnet fixes are checked by the quality control system against predefined location error and signal quality criteria and classified as "good" or "poor". Only "good" fixes that pass the criteria are used in ATDnet data products. However, it is suspected that the current ATDnet quality control system might be too conservative and that some fixes with reasonably good location accuracy are erroneously classified as poor. To examine this issue, all ATDnet good and poor fixes detected in the study area during the study period were included to the DE analysis.

The HyLMA data were obtained from the HyMeX SOP1 online database [Rison, 2012]. The ASCII data files consisted of individual HyLMA sources including their times, 3D locations (latitude, longitude and altitude), chi-squared errors and contributing stations. To avoid spurious data, all the HyLMA sources with fewer than seven contributing stations or the maximum chi-squared error more than five were excluded from the analysis.

Three storms on 5, 11 and 25 September 2012 were found to be suitable for the study. The selected storms had sufficient activity to provide good statistics, but also few enough flashes to avoid temporally coincident flashes, making individual flashes difficult to distinguish. See Table 1 for details of the storms.

TABLE I. Main Characteristics of the three Studied Storms

Date	Time UTC	Description
05/09/2012	16:30-18:10	Small localized cell.
11/09/2012	14:20-16:40	Multiple cells.
25/09/2012	09:00-14:20	Line of multiple cells.

B. Processing the HyLMA Data

The study area is located in the inner region of the area covered by the HyLMA, between 43.7°-44.5°N and 3.7°-4.7°E (Fig. 1b).

A Python script was developed to group HyLMA sources into flashes on the basis of their spatial and temporal proximity. The script returned the start and end times of HyLMA flashes and their spatial bounds. The spatial bounds were defined as boundary latitudes and longitudes of a rectangle (hereafter referred as HyLMA flash rectangle) that accommodates 98% of all HyLMA sources in an HyLMA flash. In addition flash properties including total number of HyLMA sources, maximum, minimum and average altitude of HyLMA sources, and flash area were computed. The maximum and minimum altitude of a flash was determined as the 90th and 10th percentile of all the source altitudes, respectively. The vertical extent of a flash was computed as the difference between the maximum and minimum altitude. Flash area was computed as the area of the HyLMA flash rectangle.

Next, plots of LMA sources were created for each LMA flash. Each figure included plots of latitude vs. height, longitude vs. height and latitude vs. longitude, along with a plot of the time vs. altitude evolution of a LMA flash (Fig. 2). The 3D structure of the flash could be determined from the three different 2D subplots.

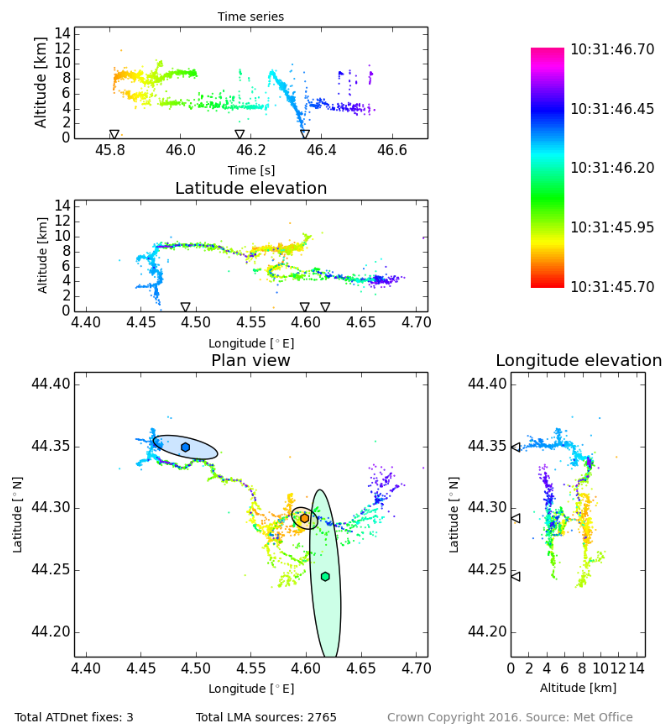

Fig. 2. An example source plot for a HyLMA CG flash detected by ATDnet. The HyLMA sources are represented as time colored dots. The coincident ATDnet fixes are depicted as triangles on the altitude plots and as hexagons with surrounding error ellipses on the plan view.

All of the plots of LMA sources were then examined visually to determine flash type. If a flash exhibited many LMA sources below 2 km with a clear time evolution of a ground channel (or channels) then it was classified as a CG. Only flashes without obvious LMA activity below 2 km were classified as IC. For some flashes that extended into low altitudes, the number of LMA sources below 2 km was rather low and/or clear time evolution of a ground channel was missing, making it difficult to determine whether a ground contact took place or not. Such LMA flashes were classified as “unclear” (U).

C. Estimating ATDnet Detection Efficiency

Two different DE values were computed in order to examine the proportion of genuine fixes that were classified as poor by the quality control system. The first is computed only using ATDnet good fixes and is called “actual” DE as it best represents the current ATDnet performance. The second DE parameter is referred as the potential DE and includes also ATDnet poor fixes that were spatially and temporally adjacent to LMA flashes, i.e. assuming perfect quality control.

LMA and ATDnet datasets were compared by first checking each LMA flash for coincident ATDnet good and poor observations. An ATDnet fix was considered to be coincident with an LMA flash if it occurred during the period from 0.1 seconds before the start of the LMA flash to 0.1 seconds after the end of the LMA flash.

All coincident ATDnet fixes were then checked spatially. If a coincident ATDnet fix was located within 8.75 km from the corresponding LMA flash rectangle then it was counted as ATDnet match. An 8.75 km buffer was chosen as it corresponds to the maximum allowed location error for ATDnet good fixes in the study area. Sometimes an ATDnet fix was located outside the 8.75 km buffer but there was an overlap between the error ellipse of the fix and the corresponding LMA flash rectangle. Such fixes were also counted as ATDnet matches but only if the major axis of their error ellipse was shorter than 100 km. The 100 km threshold prevents concurrent ATDnet fixes in distant storms with very large error ellipses being mistakenly counted as matches.

For a detailed IC DE investigation, ATDnet poor fix matches were ignored in order to represent the current ATDnet performance. ATDnet’s ability to detect an early and often vertical part of ICs – i.e. initial breakdown (IB) [Nag et al., 2009] – was examined. If an ATDnet fix existed within 0.1 seconds of the beginning of a detected IC then it was considered as initial breakdown detection. ATDnet IC DE was also studied as a function of IC altitude, vertical and horizontal extent and total number of LMA sources.

III. RESULTS

A. Flash Statistics and ATDnet DE

In total, 1915 LMA flashes were included in the study. Of these, 1341 were determined to be IC flashes and 285 were determined to be CG flashes (Table 2). The remaining 289 flashes - which constituted 15.1% of the total sample - were classified as unclear.

The overall ATDnet actual DE was approximately 91% for CGs and 24% for ICs (Table 2). CG DE ranged from 85.5% to 93.7% between the storms. For ICs, both of the more intense storms gave DE of approximately 24%. The smaller sample on 5 September 2012 gave an approximately 10% higher IC DE. The highest overall DE of 57% was observed on 5 September 2012 (Table 2). It should be noted that the overall DE is computed by using all the LMA flashes, including “unclear” flashes, as the flash type is not important here.

It came out that ATDnet potential DE was always higher than actual DE indicating that some genuine fixes were classified as poor by the quality control system. The overall potential DE was 1.4% higher for CGs and 3.7% higher for ICs. Larger difference for ICs implies that ATDnet fixes representing IC processes are more often rejected as poor fixes by the quality control system.

TABLE II. NUMBERS OF HYLMA AND ATDNET FLASHES, ATDNET ACTUAL AND POTENTIAL DE AND PERCENTAGE OF IC FLASHES FOR THE THREE STORMS STUDIED.

Date	DE Type	IC			CG			Overall			LMA IC%
		LMA	*ATDnet*	*DE*	*LMA*	*ATDnet*	*DE*	*LMA*	*ATDnet*	*DE*	
05/09/12	Actual	46	16	34.8%	41	36	87.8%	106	60	56.6%	52.9
	Potential		18	39.1%		37	90.2%		64	60.4%	
11/09/12	Actual	260	61	23.5%	55	47	85.5%	423	158	37.4%	82.5
	Potential		75	28.8%		48	87.3%		180	42.6%	
25/09/12	Actual	1035	245	23.7%	189	177	93.7%	1386	502	36.2%	84.6
	Potential		278	26.9%		179	94.7%		547	39.5%	
Total	Actual	1341	322	24.0%	285	260	91.2%	1915	720	37.6%	82.5
	Potential		371	27.7%		264	92.6%		791	41.3%	

Most of the IC detections based on one ATDnet fix whereas CGs were often represented by two or more fixes. The total number of ATDnet fixes corresponding to the 371 detected ICs was 474, i.e. 1.3 ATDnet fixes per flash. For the 264 CGs detected during the three storms 634 adjacent ATDnet fixes were found, i.e. 2.4 ATDnet fixes per flash. This indicates that ATDnet is capable of detecting not only the most powerful first return strokes of CGs but also subsequent weaker return strokes.

B. DE and IC Characteristics

For the majority of ICs registered by ATDnet, the initial breakdown was detected (Table 3). IB was often the only detected part of an IC.

It was also found that ATDnet IC DE was much higher for flashes with larger vertical extent (Fig. 3). None of the flashes vertically shorter than 1 km were detected whereas for the flashes with vertical extent over 4.5 km, DE was 45-50%. In contrast, IC DE did not appear to vary significantly with the mean altitude of the flash.

Flashes with lower minimum or higher maximum altitude were more easily detected by ATDnet (Fig. 4). The probable explanation is that ICs with higher maximum or lower minimum altitude are more likely to have a greater vertical extent which makes them more easily detectable.

The time evolution of the actual IC DE and the vertical extent of flashes were compared for the storm on 25 September 2012 (Fig. 5). There was a positive relationship between the IC DE and vertical extent of flashes with a Pearson's correlation coefficient of r=0.49 (Fig. 5b).

At the same time the relationships between IC DE and number of LMA sources as well as between IC DE and horizontal extent of flashes were less well-defined with r=0.21 and r=0.10, respectively. There was no relationship between the overall number of incoming waveforms and ATDnet IC DE (r=0.04) indicating that the system managed to process all waveforms and was not overloaded during the study period.

The mean vertical extent of ICs on 5 September was 3.5 km which is greater than 3.1 km on 11 September and 3.0 km on 25 September. This difference could explain somewhat higher IC DE for the storm on 5 September (Table 2).

TABLE III. TOTALS OF ICS AND INITIAL BREAKDOWNS (IB) DETECTED BY ATDNET AND ATDNET IB DE.

Date	ATDnet IC	ATDnet IB	IBDE
05/09/12	16	11	68.8%
11/09/12	61	51	83.6%
25/09/12	245	148	60.4%
Total	322	210	65.2%

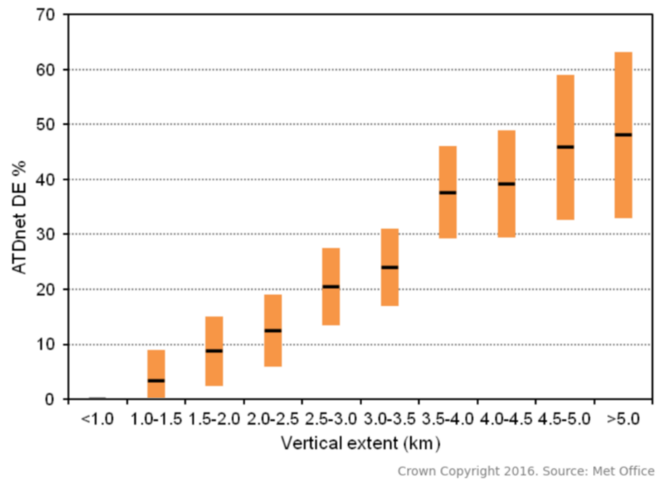

Fig. 3. ATDnet IC DE as a function of the vertical extent of the flashes (black) and its 95% confidence intervals (orange).

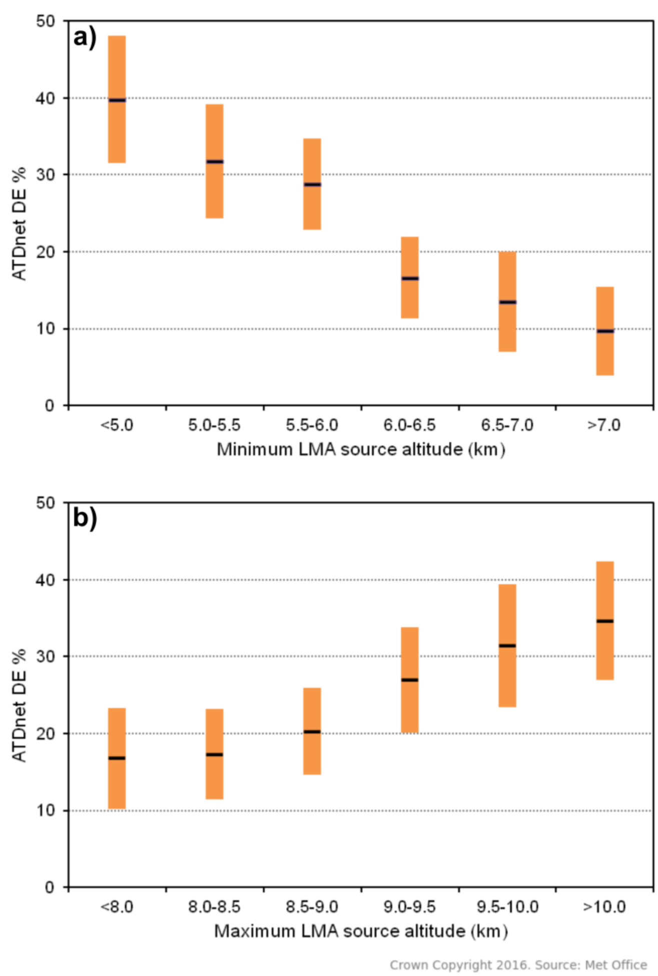

Fig. 4. ATDnet IC DE as a function of the minimum (a) and maximum (b) altitude of the flashes (black) and its 95% confidence intervals (orange).

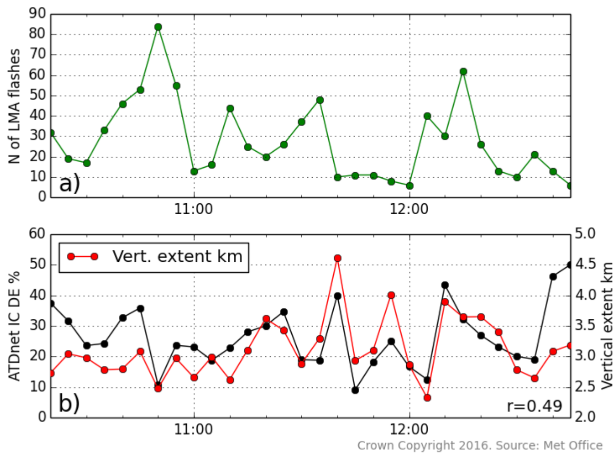

Fig. 5. Total number of HyLMA flashes (a) and ATDnet IC DE vs. vertical extent of HyLMA flashes for 5-minute time bins during 1020-1250 UTC on 25 September 2012. The black line represents ATDnet IC DE (b).

IV. Discussion

ATDnet actual CG DE was found to be 91% (Table 2) for the storms analysed in this study, which is an excellent result for a long-range LLS. For comparison, the Vaisala GLD360 system is estimated to detect 86-92% CGs over the continental United States [Demetriades et al., 2010], ZEUS was found to be capable of detecting approximately 25% of CGs over Central-Western Europe [Lagouvardos et al., 2009] and WWLLN DE was estimated to be 10.3% over the contiguous U.S. in 2009 [Abarca et al., 2010].

On the basis of the current ATDnet configuration (locations of sensors) it can be assumed that the performance demonstrated in this analysis is representative of large areas within the perimeter of ATDnet including Central and Western Europe. Small spatial variations in DE due to surface features such as mountains are probable over the whole ATDnet range but it is not possible to estimate their impact on the basis of one study area.

However, it should be taken into account that all three storms analyzed in the present paper occurred during the daytime. ATDnet DE is expected to be lower at night due to modal interference between sky wave propagation modes 1 and 2 [Bennett et al., 2011]. Thus, inclusion of nighttime storms would probably result in somewhat lower DE.

As ATDnet operational sensors are located in and around Europe, its DE is expected to gradually decrease with increasing distance from Europe. Thus, there are large areas in the world where “global” networks like GLD360 and WWLLN are expected to perform better than ATDnet. A comparison with those networks might be of benefit in the future to more precisely quantify the spatial range of ATDnet.

The results revealed that ATDnet actual IC DE was 24%. It is known that other VLF systems such as WWLLN [Rodger et al., 2006] and ZEUS [Lagouvardos et al., 2009] also detect some cloud lightning but their exact IC DE is not available. Sufficiently sensitive short-range networks are capable of detecting more ICs than ATDnet as their shorter baselines between sensors can more easily detect IC radio emissions that are generally weaker. For example NLDN DE has reported to be 30-58% for ICs [Murphy et al., 2014].

It was demonstrated that the performance of the current quality control system is generally good with only 3.7% of potential flash detections rejected as poor fixes. Notably 49 ICs and only 4 CGs were rejected as poor fixes (Table 2). This clearly indicates that weaker IC sferics more often lead to fixes that fail to pass the quality control. On the basis of those findings it can be said that improvements in the quality control system would allow somewhat higher DE.

The analysis showed that initial breakdown DE was as high as 65% for the detected ICs (Table 3). This is in line with the fact that the largest radio emissions of cloud lightning are associated with IB process [Rakov and Uman, 2003].

Flashes with greater vertical extent were more easily detected (Fig. 3 and 5). The relationship between vertical extent and DE is in line with the fact that the vertical whip antennas used by ATDnet sensors are expected to favor detection of vertically polarized signals. Long vertical channels of ICs probably result in stronger vertically polarized sferics that are able to trigger the sensors far enough to meet the four contributing sensor criteria necessary for ATDnet fix location.

It is also likely that vertically extensive ICs are more powerful as the positive and negative charge regions in a thundercloud are further apart and stronger charges are needed to generate electric field strong enough to exceed the resistance of the air between the charge regions. The resulting ICs are more powerful and larger amount of charge is transferred via the vertical channel. A stronger vertical channel in turn emits more powerful sferics.

Changes in lightning location network DE are usually assumed to be associated with changes in the network (e.g. change in the network geometry or number of sensors). This study demonstrated that IC DE is also significantly affected by flash characteristics and varies between the individual storms (Table 2) but also during the same storm (Fig. 5). DE variations were in fact much larger in the course of the same storm than between the three storms.

A wider study with more storms is required to further investigate the relationship between IC properties and DE. Such a study should also include nighttime storms to estimate the influence of changes in propagation conditions in the wider diurnal scale. It would also be interesting to include other European lightning location networks. This would give invaluable information about the capabilities and limitations of different short-range and long-range detection methods.

V. Conclusions

The Met Office ATDnet long-range VLF lightning location system was validated against the HyLMA deployed in the south of France as part of the HyMeX project Special Observation Period 1. The results revealed that ATDnet DE for daytime CGs was 91% which is quite high for a long-range LLS.

It was also confirmed that ATDnet is capable of detecting ICs. This is an important ability as it allows locating storms with low or no CG activity.

The results revealed that the performance of the current quality control system is generally good with only 3.7% of potential flash detections rejected as poor fixes. However, this finding also indicates that improvements in the quality control procedures could allow somewhat higher DE.

The most important finding about IC detection is that DE is related to the vertical extent of ICs and not to the overall amount of incoming waveforms. This indicates that DE is controlled by flash characteristics and the system was not overloaded by incoming waveforms. A more comprehensive study with a larger data sample would be needed to better understand the relationship between flash characteristics and ATDnet detection efficiency.

ACKNOWLEDGMENT

The LMA data were obtained from the HyMeX program, sponsored by Grants MISTRALS/HyMeX and ANR-11-BS56-0005 IODA-MED project. We thank Eric Defer for his useful comments and suggestions in the early stage of the study.

REFERENCES

Abarca, S. F., K. L. Corbosiero, and T. J. Galarneau (2010), An evaluation of the Worldwide Lightning Location Network (WWLLN) using the National Lightning Detection Network (NLDN) as ground truth, J. Geophys. Res. Atmospheres, 115(D18).

Anderson, G., and D. Klugmann (2014), A European lightning density analysis using 5 years of ATDnet data, Nat. Hazards Earth Syst. Sci., 14, 815–829, doi:10.5194/nhess-14-815-2014.

Bennett, A. J., C. Gaffard, J. Nash, G. Callaghan, and N. C. Atkinson (2011), The effect of modal interference on VLF long-range lightning location networks using the waveform correlation technique, J. Atmos. Oceanic Technol., 28(8), 993–1006, doi:10.1175/2011JTECHA1527.1.

Betz, H. D., K. Schmidt, P. Laroche, P. Blanchet, W.P. Oettinger, E. Defer, Z. Dziewit, and J. Konarski, 2009: LINET—An international lightning detection network in Europe, Atmos. Res. 2009, 91 (2), 564–573.

Biagi, C. J., K. L. Cummins, K. E. Kehoe, and E. P. Krider (2007), National Lightning Detection Network (NLDN) performance in southern Arizona, Texas, and Oklahoma in 2003-2004, J. Geophys. Res. Atmospheres, 112(D5), doi:10.1029/2006JD007341.

Cummins, K., and M. Murphy (2009), An overview of lightning locating systems: History, techniques, and data uses, with an in-depth look at the U.S. NLDN, IEEE Trans. Electromagn. Compat., 51(3), 499–518, doi:10.1109/TEMC.2009.2023450.

Defer, E., et al. (2015), An overview of the lightning and atmospheric electricity observations collected in Southern France during the HYdrological cycle in Mediterranean EXperiment (HyMeX), Special Observation Period 1, Atmos. Meas. Tech., 8, 649–669, doi: 456 10.5194/amt-8-649-2015.

Demetriades, N. W., M. J. Murphy, and J. A. Cramer (2010), Validation of Vaisalas Global Lightning Dataset (GLD360) over the continental United States, paper presented at 21st International Lightning Detection Conference & 3rd International Lightning Meteorology Conference, Orlando, Florida.

Dentel, L. M., B. R. P. da Rocha, and J. R. S. de Souza (2014), Evaluation of STARNET lightning detection performance in the Amazon region, Int. J. Remote Sens., 35(1), 115–126, doi:10.1080/01431161.2013.862604.

Drobinski, J., P.and Font, J. Tintoré, and H. Wernli (2014), HyMeX: A 10-year multidisciplinary program on the Mediterranean water cycle, Bull. Amer. Meteor. Soc., 95, 1063–1082, doi:10.1175/BAMS-D-12-00242.1.

Enno, S. E., G. Anderson, and J. Sugier (2016), ATDnet detection efficiency and cloud lightning detection characteristics from comparison with the HyLMA during HyMeX SOP1, J. Atmos. Oceanic Technol., manuscript under revision.

Jacobson, A. R., R. Holzworth, J. Harlin, R. Dowden, and E. Lay (2006), Performance assessment of the World Wide Lightning Location Network (WWLLN), using the Los Alamos Sferic Array (LASA) as ground truth, J. Atmos. Oceanic Technol., 23(8), 1082–1092, doi:10.1175/JTECH1902.1.

Krehbiel, P. R., R. J. Thomas, W. Rison, T. Hamlin, J. Harlin, and M. Davis (2000), GPS-based mapping system reveals lightning inside storms, Eos, Trans. Amer. Geophys. Union, 81(3), 21–25, doi:10.1029/00EO00014.

Lagouvardos, K., V. Kotroni, H.-D. Betz, and K. Schmidt (2009), A comparison of lightning data provided by ZEUS and LINET networks over Western Europe, Nat. Hazard Earth Sys., 9(5), 1713–1717, doi:10.5194/nhess-9-1713-2009.

Lay, E. H., R. H. Holzworth, C. J. Rodger, J. N. Thomas, O. Pinto, and R. L. Dowden (2004), WWLL global lightning detection system: Regional validation study in Brazil, Geophys. Res. Lett., 31(3), doi:10.1029/2003GL018882.

Murphy, M. J., A. Nag, J. A. Cramer, and A. E. Pifer (2014), Enhanced cloud lightning performance of the US National Lightning Detection Network following the 2013 upgrade, paper presented at 23rd International Lightning Detection Conference & 5th International Lightning Meteorology Conference, Tuscon, Arizona.

Nag, A., B. A. DeCarlo, and V. A. Rakov (2009), Analysis of microsecond- and submicrosecond-scale electric field pulses produced by cloud and ground lightning discharges, Atmos. Res., 91(2), 316–325.

Nag, A., et al. (2011), Evaluation of U.S. National Lightning Detection Network performance characteristics using rocket-triggered lightning data acquired in 2004-2009, J. Geophys. Res. Atmospheres, 116(D2), doi:10.1029/2010JD014929.

Nag, A., M. J. Murphy, W. Schulz, and K. L. Cummins (2015): Lightning locating systems: Insights on characteristics and validation techniques, Earth and Space Science, 2(4), doi: 509 10.1002/2014EA000051.

Poelman, D. R., F. Honoré, G. Anderson, and S. Pedeboy (2013a), Comparing a regional, subcontinental, and long-range lightning location system over the Benelux and France, J. Atmos. Oceanic Technol., 30(10), 2394–2405, doi:10.1175/JTECH-D-12-00263.1.

Poelman, D. R., W. Schulz, and C. Vergeiner (2013b), Performance characteristics of distinct lightning detection networks covering Belgium, J. Atmos. Oceanic Technol., 30(5), 942–951, doi:10.1175/JTECH-D-12-00162.1.

Rakov, V. (2013), Electromagnetic methods of lightning detection, Surv. Geophys., 34(6), 731–753, doi:10.1007/s10712-013-9251-1.

Rakov, V. A., and M. A. Uman (2003), Lightning: physics and Effects, Cambridge Univ. Press, New York.

Rison, W. (2012), HyMeX Lightning Mapping Array. New Mexico Tech, http://dx.doi.org/10.6096/MISTRALS-HYMEX.LIGHTNING.LMA (last access: 8 February 2016).

Rison, W., R. J. Thomas, P. R. Krehbiel, T. Hamlin, and J. Harlin (1999), A GPS-based three-dimensional lightning mapping system: Initial observations in central New Mexico, Geophys. Res. Lett., 26(23), 3573–3576, doi:10.1029/1999GL010856.

Rodger, C. J., S. Werner, J. B. Brundell, E. H. Lay, N. R. Thomson, R. H. Holzworth, and R. L. Dowden (2006), Detection efficiency of the VLF World-Wide Lightning Location Network (WWLLN): initial case study, Ann. Geophys., 24(12), 3197–3214.

Said, R. K., U. S. Inan, and K. L. Cummins (2010), Long-range lightning geolocation using a VLF radio atmospheric waveform bank, J. Geophys. Res. Atmospheres, 115(D23), doi:10.1029/534 2010JD013863.